# Anomalous Hall effect based on Pt/$Bi_{0.9}La_{0.1}FeO_3$ bilayers



2016 Jpn. J. Appl. Phys. 55 045801

(http://iopscience.iop.org/1347-4065/55/4/045801)

Japanese Journal of Applied Physics **55**, 045801 (2016)
http://doi.org/10.7567/JJAP.55.045801

**REGULAR PAPER**

# Anomalous Hall effect based on $Pt/Bi_{0.9}La_{0.1}FeO_3$ bilayers

Rongli Gao[1,2*], Chunlin Fu[1,2], Wei Cai[1,2], Gang Chen[1,2], Xiaoling Deng[1,2], Hongrui Zhang[3], Jirong Sun[3], and Baogen Shen[3]

[1]*School of Metallurgy and Materials Engineering, Chongqing University of Science and Technology, Chongqing 401331, China*
[2]*Chongqing Key Laboratory of Nano/Micro Composite Materials and Devices, Chongqing 401331, China*
[3]*Beijing National Laboratory for Condensed Matter Physics and Institute of Physics, Chinese Academy of Science, Beijing 100190, China*

*E-mail: gaorongli2008@163.com

Received October 16, 2015; revised December 17, 2015; accepted December 23, 2015; published online March 2, 2016

A 2.5-nm-thick platinum film with the shape of a Hall bar was deposited by magnetron sputtering on weak ferromagnetic rhombohedral and tetragonal $Bi_{0.9}La_{0.1}FeO_3$ thin films. An anomalous Hall effect (AHE) was observed and studied as a function of magnetic field ($H$) and temperature ($T$). For the two samples, besides the obvious difference in the anomalous Hall resistance, the anomalous Hall resistance increases sharply with decreasing temperature, and even changes sign, thus violating the conventional expression. This observation indicates strong proximity effects and local-field-induced magnetic ordering in Pt on weak ferromagnetic thin films of rhombohedral and tetragonal $Bi_{0.9}La_{0.1}FeO_3$ and their contribution to the spin-related measurements should not be neglected. 

## 1. Introduction

The Hall effect, which is a useful tool for probing charge transport properties and material types in the solid state,[1–3] has attracted a considerable amount of attention for many years not only due to its widespread application in magnetic field sensors but also because of its wealth of new phenomena, such as the integer and fractional quantum Hall effects, the anomalous Hall effect, and the spin-dependent Hall effect.[2–4] In analogy to the conventional Hall effect, the anomalous Hall effect has been proposed to occur in magnetic systems as a result of spin–orbit interaction, and definitive progress has been achieved in understanding the mechanisms in homogeneous metals and metallic alloys in recent years.[5] It is known that the Hall resistivity $\rho_H$ in a ferromagnet[2–4] has some extra contribution originating from spontaneous magnetization and can be fitted by

$$\rho_H = R_0 B + 4\pi R_s M, \quad (1)$$

where $R_0$ is the usual Hall coefficient and $R_s$ is the anomalous Hall coefficient. The anomalous Hall effect (AHE $= 4\pi R_s M$) has been useful in the investigation and characterization of itinerant electron ferromagnets.[6]

It is assumed from formula (1) that the anomalous contribution is proportional to the magnetization $M$, taking into consideration the fact that the magnetization $M$ has a nonmonotonic dependence on the magnetic field $H$; therefore, the anomalous contribution in the Hall effect should also vary nonmonotonically with $H$. However, some researchers have found a nonmonotonic dependence on $H$ that even includes a sign change, which gives an important clue to the origin of the AHE. Most theories regard the AHE to have extrinsic origins that involve processes such as skew scattering[7] and side-jump mechanisms.[8] In contrast, several works[2,9–12] regard the AHE to have an intrinsic origin and this intrinsic AHE has been reinterpreted in terms of the Berry curvature of the occupied Bloch states.[13,14]

Generally, the intrinsic AHE is evaluated numerically in ferromagnetic materials.[15–17] However, it was reported that, in addition to magnetic materials, the AHE can also be observed in nonmagnetic materials by using an external electrical or magnetic field.[18–21] Of all the nonmagnetic metals, platinum (Pt) metal has been employed most often because it plays an essential role in generating and detecting a pure spin current. Given the prominent role of Pt in spin-based phenomena, it is imperative to ascertain the transport and magnetic characteristics of thin Pt films in contact with a ferrimagnet. When a thin Pt film is deposited on a ferrimagnetic insulator, its conducting properties can be determined through its magnetotransport properties. Thus, to further elucidate this phenomenon and mechanism, it is of critical importance to ascertain whether one can observe the AHE when Pt is grown on a weak magnet, such as an antiferrimagnetic (AFM) material.

Among AFM materials, $BiFeO_3$ (BFO) is typical not only because of its weak magnetism but also because of its robust polarization ($\sim 100\,\mu C/cm^2$) above room temperature.[22–24] On one hand, most of the previous works focus on nonmagnetic metal/ferromagnetic insulator bilayers, but investigations on weak magnetic materials are rare. It is uncertain whether the nonmagnetic metal Pt grown on BFO can also show magnetic behavior and whether the AHE can be observed. On the other hand, some works have reported the AHE based on electric-field-induced Pt films,[25,26] which is ascribed to the strong spin–orbit coupling effect in Pt. It should be pointed that the local electric field near the face of BFO films can be estimated to be $\sim 5000\,MV/cm$ using the formula $E = \sigma/2\varepsilon_0$ for an infinite plate without considering the screen effect. $\sigma$ and $\varepsilon_0$ are the charge density of the BFO film surface ($\sim 100\,\mu C/cm^2$) and the permittivity of vacuum, respectively. In the case of electric field (gate) tuning of the AHE, the electric double layer (EDL) was found to work as a nanogap capacitor with an electric field of $\sim 27\,MV/cm$, which is 4.6 times greater than the intrinsic electric field of a Au surface, by applying 1.7 V of positive (negative) gate voltage. Apparently, the field near the BFO face is at least two orders of amplitude larger than the above-mentioned value. For this reason, we believe that an AHE should exist when Pt is grown on a BFO film. It was reported that rhombohedrally distorted perovskite BFO shows a robust ferroelectricity of $100\,\mu C/cm^2$ when it is a metastable tetragonal phase with a giant axial ratio ($\sim 1.27$) and an extremely large spontaneous polarization of $\sim 150\,\mu C/cm^2$. Consequently, the difference in the polarization will induce different local electric fields and, in turn, cause diverse results.

On the basis of the above consideration, in this work, we report an electrical transport study of thin Pt films on AFM semiconductors, on both rhombohedral $Bi_{0.1}La_{0.9}FeO_3$ (R-BLFO) and tetragonal $Bi_{0.1}La_{0.9}FeO_3$ (T-BLFO) thin films. Herein, La doping is for the sake of reducing the leakage current of BFO and hence obtaining the preferred film. We have observed a nonmonotonic dependence of AH resistivity on the temperature and magnetization, including a sign change at around room temperature. Rather than the more complex description using the intrinsic Hall effect, however, all the features observed can be interpreted using a simple model of bilayers consisting of nonmagnetic and magnetic Pt films by taking into consideration the magnetic proximity effects (MPE)[27,28] or local-electric-field induced magnetic characteristics in such Pt thin films. These results raise questions about the suitability of using Pt in establishing pure spin current phenomena and of tuning the Hall effect by manipulating the electric field using ferroelectric materials.

## 2. Experimental procedure

Patterned Pt thin films with a thickness of ~2.5 nm have been deposited by magnetron sputtering on epitaxial R-BLFO and T-BLFO films. The BLFO thin films with a thickness of ~40 nm were grown epitaxially on (001)-oriented $LaAlO_3$ (LAO) substrates at 650 °C. By controlling the deposition oxygen pressure, one can obtain R-like and T-like BLFO films. The other deposition parameters are depicted in detail elsewhere.[29,30] The nominal thicknesses of the individual layers were calculated from the sputtering time and rate. The structural characterization of the BLFO films was performed by X-ray diffraction (XRD) using the M/s Bruker D8-Discover X-ray diffractometer with Cu K$\alpha_1$ radiation. To perform Hall and resistance measurements simultaneously and to guarantee that the data for electrical transport (Hall and longitudinal resistivity) measurements were obtained from the same sample, masks were used to make patterned samples. Transport measurements were carried out with Quantum Design PPMS-14H at 300–2 K. The magnetization of all samples was measured with MPMS-XL, and the residual longitudinal offset in the measured Hall voltage was excluded on the basis of its different symmetry against the magnetic field, $H$, and the anomalous part ($\rho_{xy}$) of the Hall resistivity was extracted using Eq. (1). The samples for X-ray diffraction, surface morphology, and transport measurements have dimensions of $10 \times 10 \times 0.5\,mm^3$.

## 3. Results and discussion

Normal XRD $\theta$–$2\theta$ scans provide information on the crystal orientation in an out-of-plane direction and the corresponding lattice parameter. As shown in Fig. 1(a), the BLFO films on the LAO substrate reveal high-quality, epitaxial films that appear to be a single phase. An appreciable shift of the BLFO (00l) diffraction peak is observed with these two films. The out-of-plane $c$ parameters for R-BLFO and T-BLFO films are 0.397 and 0.451 nm, respectively. Figure 1(b) shows the crystal structure of R-BLFO (bulk BFO is a rhombohedrally distorted perovskite with a space group of $R3c$ and a pseudocubic lattice parameter $a$ of ~0.396 nm and $c/a \sim 1.02$)[31] and T-BLFO (the unit cell has a high tetragonality $c/a \sim 1.26$).[32] Clearly, elongation greater than 10% along the

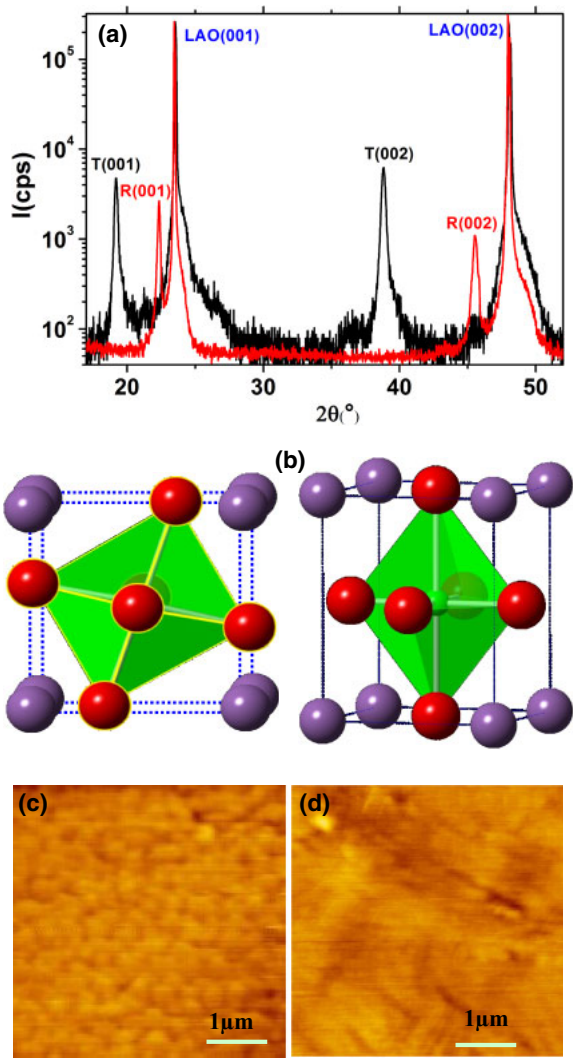


**Fig. 1.** (Color online) (a) XRD spectra of rhombohedral and tetragonal BLFO films grown on $LaAlO_3$ substrates. (b) shows crystal structures of R-BLFO and T-BLFO. Atomic force microscopy surface topographies of representative (c) T-BLFO and (d) R-BLFO films for scanning area of $5 \times 5\,\mu m^2$.

$c$-axis direction compared with R-BFO would induce significant changes in most physical properties. The BLFO layers have a top surface root mean square roughness of less than 0.3 nm over a scanning area of $5 \times 5\,\mu m^2$, as characterized by atomic force microscopy [Figs. 1(c) and 1(d)].

The temperature dependences of the sheet resistance $R_{xx}$ values of the Pt thin films grown on R-BLFO and T-BLFO were compared. As shown in Fig. 2(a), both series samples exhibit very similar temperature dependences. The inset of Fig. 2(a) is a schematic diagram of the patterned Hall bar on a substrate in the $xy$ plane with $H$ perpendicular to this plane. In addition, the resistivity of the Pt thin film sample decreases gradually with decreasing temperature, but a nonmonotonic temperature dependence becomes obvious and a resistivity minimum appears at around 20 K. $R_{xx}$ indicates insulating characteristics ($dR_{xx}/dT < 0$) in the low-temperature region (below ~20 K). This occurrence of the metal-to-insulator transition in the Pt thin-film sample should originate from the weak localization of electrons caused by the dimensional effect. Quantitative analysis of the insulating resistance results shows that $R_{xx}$ changes linearly with $\ln T$ at low

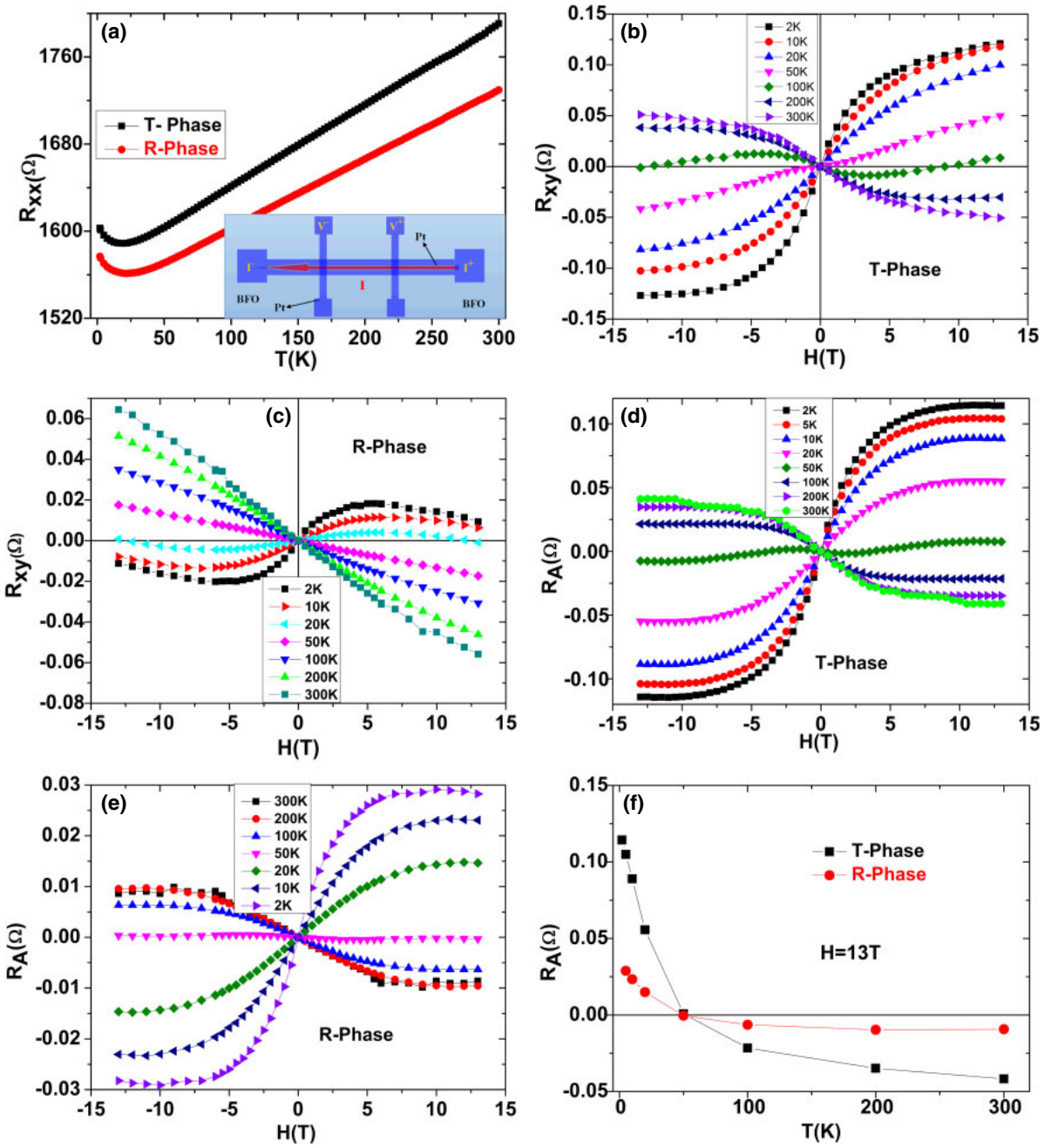


**Fig. 2.** (Color online) (a) Dependence of temperature on sheet resistance $R_{xx}$ on R-BLFO and T-BLFO. The inset in (a) is the schematic diagram of the patterned Hall bar on a substrate in the $xy$ plane with $H$ perpendicular to this plane. Representative field-dependent Hall resistivity curves measured at different temperatures on (b) Pt/T-BLFO and (c) Pt/R-BLFO. Temperature-dependent anomalous Hall resistivity for the (d) Pt/R-BLFO and (e) Pt/T-BLFO films. (f) AHE resistance $R_A$ for both Pt/R-BLFO and Pt/T-BLFO films in the field of 13 T as a function of temperature.

temperatures. This phenomenon can be ascribed to the two-dimensional (2D) weak disorder-induced electron localization (EL) and/or 2D Coulomb interaction (CI).[33)]

Magnetic field dependences of the Hall resistivity $R_{xy}$ values at various temperatures for all samples are shown in Figs. 2(b) and 2(c). In both films, we observed a large AHE signal derived from the spontaneous magnetization. It was difficult to determine the ordinary and anomalous Hall resistivities because the resistivity varies nonmonotonically with $T$, and even changes sign. The ordinary Hall coefficient $R_H^O = dR_{xy}/dH$ from the slopes for the two samples shows a dependence on temperature and field (the slope differs with temperature and magnetic field); the slope of T-BFO varies with temperature and even changes sign at about 100 K, but does not change sign in high field. The S-like feature in the Hall curves in Fig. 2 at intermediate temperatures, such as below 100 K, implies that the AHE is composed of positive and negative components with different saturation magnetic fields. Therefore, the Hall resistance should consist of three components: the ordinary Hall resistivity, a positive component, and a negative component. The contribution of the anomalous Hall resistivity $R_A$ is estimated as the deviation of $R_{xy}$ from $R_O$. From the field-dependent anomalous Hall resistivity curves, we take 13 T as the saturated anomalous Hall resistivity. Figures 2(d) and 2(e) show the temperature-dependent anomalous Hall resistivities for the Pt/R-BLFO and Pt/T-BLFO films, respectively. Both an ordinary Hall effect and an AHE, where the latter is another key magnetic

characteristic, are seen. The AHE resistance $R_A$ for both Pt/R-BLFO and Pt/T-BLFO films at the field of 13 T increase sharply with decreasing temperature, and even changes sign at about 50 K, as shown in Fig. 2(f). Such behaviors are sometimes observed in other ferromagnetic materials.[27,28] Once again, there is a stark contrast between Pt/R-BLFO and Pt/T-BLFO films. The Hall resistivity for Pt/T-BLFO always increases with magnetic field at low and high temperatures, as shown Fig. 2(b), whereas it approaches saturation at ~6 T for Pt/R-BLFO at low temperature, as can be seen in Fig. 2(c). This is, the anomalous Hall resistivity can be saturated in higher field. Furthermore, the AHE resistance for Pt/T-BLFO is almost one order higher than that for Pt/R-BLFO. Unexpectedly, the AHE in Pt/R-BLFO and Pt/T-BLFO exhibits very similar behaviors to that of field-dependent magnetization [see Fig. 3(a)] if only the magnitude is considered. One can see from Fig. 3(a) that the magnetization of T-BLFO is somewhat larger than that of R-BLFO, and that the $M$–$H$ curve of T-BLFO seems more difficult to become saturated than that of R-BLFO films. Therefore, if the magnetization of BLFO is the key factor behind the AHE, the anomalous part of the Hall effect in Pt/T-BLFO should be larger than that of Pt/T-BLFO; this is consistent with our results. In contrast, the $M$–$H$ curve of T-BLFO seems more difficult to become saturated than that of R-BLFO films, which is in accordance with the variation tendency of the $R_{xy}$–$H$ curves shown in Fig. 2. It should be pointed that, although the BLFO films are not insulators, their resistivity is far larger than that of Pt films; hence, the measured Hall resistivity can be fully attributed to Pt metal. For thin films of soft ferromagnetic materials, such as Fe and Gd, the magnetization preferably lies in the film plane owing to the strong demagnetizing effect. When a magnetic field is applied perpendicular to the film plane, the magnetization is forced to align with the field direction. Therefore, the magnetization in the field direction is proportional to the field strength until the magnetization is fully aligned in the field direction at about 18 and 20 kOe for Fe and Gd films, respectively. This process leads to a linear dependence of magnetization on the magnetic field in the low-field range and saturation in the high-field range. Because of the linear dependence of the AHE resistivity on magnetization [Eq. (1)], a steep change in the AHE resistivity is observed at low fields and saturation at high fields.

It has been reported that a Pt thin film grown on an insulating ferrimagnetic $Y_3Fe_5O_{12}$ (YIG) can show AHE behaviors, and it was assumed that these ferromagnet-like characteristics strongly indicate strong proximity effects and induce magnetic ordering in Pt on magnetic insulators. The study results further suggested that the induced Pt moments are located within 1 nm from the interface.[34] Therefore, considering the fact that the R-BLFO underlayer and the T-BLFO substrates have nearly the same surface roughness, the AHE resistivity reduction of the Pt layers should not originate from the thin-film uniformity. The introduction of magnetic ordering in Pt by the BLFO underlayer will result in band splitting for the Pt 5d spin-up and spin-down electrons, which will in turn lower the density of states (DOS) at the Pt Fermi level. The reduction in the DOS results in less s-d scattering and leads to a lower resistivity for the magnetically ordered Pt layer. Therefore, a comparison of the Pt film resistivities of Pt/T-BLFO and Pt/R-BLFO films also suggests that the electronic structure of the Pt layer has been appreciably modified by the BLFO underlayer. Hence, we argue that the different Hall effect behaviors in our two samples may result from the different proximity effects between Pt/R-BLFO and Pt/T-BLFO interfaces.

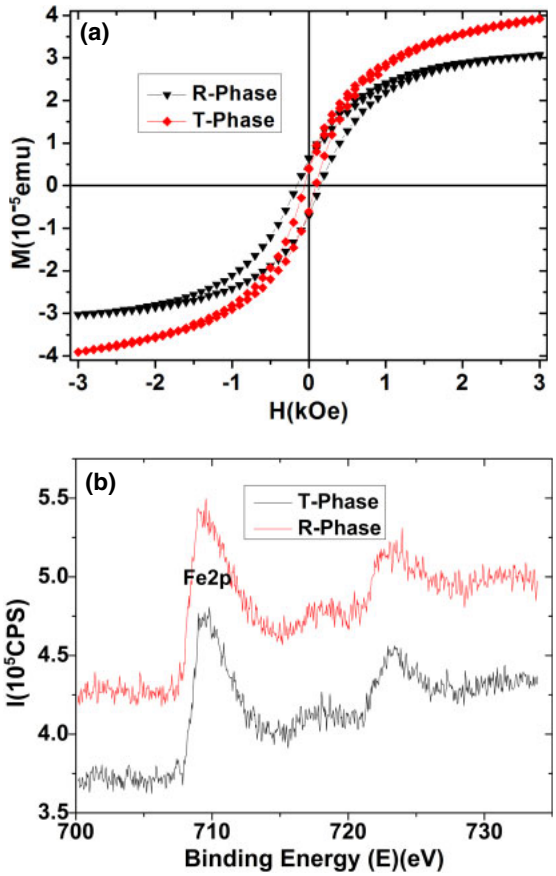


**Fig. 3.** (Color online) (a) Magnetic hysteresis loop at 300 K of R-BLFO and T-BLFO films as a function of magnetic field $H$ applied in-plane. (b) XPS results for Fe 2p on the surface of T-BLFO and R-BLFO films.

In order to elucidate how this happens and considering the fact that Pt is magnetized as a result of the magnetic proximity effect, the intensity of Fe 2p at the surface of the two samples T-BLFO and R-BLFO films was measured by XPS and is shown in Fig. 3(b). One can conclude from Fig. 3(b) that the Fe 2p intensities for T-BLFO and R-BLFO are different, and that the density of Fe in T-BLFO is lower than that in R-BLFO films. Unfortunately, this result cannot explain the observed difference in the AHE between Pt/R-BLFO and Pt/T-BLFO films at all if the AHE is attributed to different proximity effects between Pt/R-BLFO and Pt/T-BLFO interfaces. In addition, if the AHE originates from the proximity effect, one cannot observe the sign change of the anomalous Hall part because the magnetization should vary monotonically with magnetic field.

Therefore, the origin of the anomalous Hall resistance in nonmagnetic Pt metal at least is not attributable to the magnetized Pt as a result of the proximity effect. Considering the sign change of the Hall resistivity, the AHE is composed of positive and negative components with different saturation magnetic fields. Therefore, the Hall resistance should consist of three components, i.e., the ordinary Hall resistivity, a positive component, and a negative component. We suppose

that the observed RH may stem from the AHE in a paramagnet with local magnetic moments. It is known that not only uniform long-range magnetic order but also local magnetic moments can contribute to the AHE.[35,36] Superparamagnetic moments have been reported to induce the AHE in Co-doped $TiO_2$[35] and Pt thin films embedded with Fe nanoparticles.[36] The mechanism of the induced local moments in the BLFO/Pt film remains the subject of ongoing investigation. A possible scenario is that polarization on the Pt channel induces ferromagnetism in a manner similar to that in the case of gate (electric field)-tuned thin films of Pt.[25] As a result, we believe that the polarization of BLFO films may also produce local electric fields at the interface of Pt, which might generate local magnetic moments in Pt owing to its large spin–orbit interaction. Also, possible structural disorder in the Pt film would prohibit long-range order of ferromagnetism, resulting in large local moments, as observed in superparamagnetic systems. The difference in Hall effect between T-BLFO/Pt and R-BLFO/Pt films may originate from (i) the different magnetizations induced by BLFO films as a result of the proximity effect; (ii) the difference in the local electric field between the BLFO and Pt interface, which induces different spin–orbit interactions of nonmagnetic Pt metal, which in turn gives rise to various local magnetic moments in Pt.

## 4. Conclusions

We studied the electrical transport characteristics of thin Pt films on both antiferromagnetic semiconductor rhombohedral and tetragonal $Bi_{0.9}La_{0.1}FeO_3$ thin films. For the two samples, besides the obvious difference in the AHE resistance $R_A$, the AHE increases sharply with decreasing temperature and even changes sign, thus violating the conventional expression. This phenomenon can be explained by the bilayers that consist of nonmagnetic and magnetic layers. This observation indicates strong proximity effects and local-field-induced magnetic ordering in Pt on weak ferromagnetic $Bi_{0.9}La_{0.1}FeO_3$ thin films. Pt metal, being nonmagnetic and having a strong spin–orbit coupling interaction, has been instrumental in detecting the pure spin current and establishing most of the recent spin-based phenomena. The suitability and unique role of Pt on antiferromagnets for detecting the pure spin current have been compromised. As a result, the pure spin current detected by a thin Pt layer is tainted with a spin-polarized current. Our result may be useful in tuning the Hall effect by an external electric field formed by manipulating the ferroelectric polarization.

## Acknowledgements

The present work has been supported by the the Knowledge Innovation Project of the Chinese Academy of Sciences, the Beijing Municipal Natural Science Foundation, the National Natural Science Foundation of China (Grant Nos. 51102288, 51372283, 51402031, and 61404018), the Natural Science Foundation Project of CQ (CSTC2012jjA50017), and the cooperative project of the Academician Workstation of Chongqing University of Science and Technology (CKYS2014Z01 and CKYS2014Y04).

1) E. H. Hall, Philos. Mag. **12**, 157 (1881).
2) T. Jungwirth, Q. Niu, and A. H. MacDonald, Phys. Rev. Lett. **88**, 207208 (2002).
3) Y. Tian, L. Ye, and X. Jin, Phys. Rev. Lett. **103**, 087206 (2009).
4) S. R. Shinde, S. B. Ogale, J. S. Higgins, H. Zheng, A. J. Millis, V. N. Kulkarni, R. Ramesh, R. L. Greene, and T. Venkatesan, Phys. Rev. Lett. **92**, 166601 (2004).
5) Y. K. Kato, R. C. Myers, A. C. Gossard, and D. D. Awschalom, Science **306**, 1910 (2004).
6) L. Q. Liu, C. F. Pai, Y. Li, H. W. Tseng, D. C. Ralph, and R. A. Buhrman, Science **336**, 555 (2012).
7) S. Geprägs, S. Meyer, S. Altmannshofer, M. Opel, F. Wilhelm, A. Rogalev, R. Gross, and S. T. B. Goennenwein, Appl. Phys. Lett. **101**, 262407 (2012).
8) L. Berger, Phys. Rev. B **2**, 4559 (1970).
9) R. Karplus and J. M. Luttinger, Phys. Rev. **95**, 1154 (1954).
10) J. W. Ye, Y. B. Kim, A. J. Millis, B. I. Shraiman, P. Majumdar, and Z. Tešanović, Phys. Rev. Lett. **83**, 3737 (1999).
11) Y. Taguchi, Y. Ohara, H. Yoshizawa, N. Nagaosa, and Y. Tokura, Science **291**, 2573 (2001).
12) Y. Lyanda-Geller, S. H. Chun, M. B. Salamon, P. M. Goldbart, P. D. Han, Y. Tomioka, A. Asamitsu, and Y. Tokura, Phys. Rev. B **63**, 184426 (2001).
13) Z. Fang, N. Nagaosa, K. S. Takahashi, A. Asamitsu, R. Mathieu, T. Ogasawara, H. Yamada, M. Kawasaki, Y. Tokura, and K. Terakura, Science **302**, 92 (2003).
14) D. Xiao, M. C. Chang, and Q. Niu, Rev. Mod. Phys. **82**, 1959 (2010).
15) Y. G. Yao, L. Kleinman, A. H. MacDonald, J. Sinova, T. Jungwirth, D. S. Wang, E. Wang, and Q. Niu, Phys. Rev. Lett. **92**, 037204 (2004).
16) N. Vlietstra, J. Shan, V. Castel, J. Ben Youssef, G. E. W. Bauer, and B. J. van Wees, Appl. Phys. Lett. **103**, 032401 (2013).
17) S. H. Chun, M. B. Salamon, Y. L. Geller, M. Goldbart, and P. D. Han, Phys. Rev. Lett. **84**, 757 (2000).
18) A. Fernández-Pacheco, J. M. De Teresa, J. Orna, L. Morellon, P. A. Algarabel, J. A. Pardo, and M. R. Ibarra, Phys. Rev. B **77**, 100403(R) (2008).
19) S. Sangiao, L. Morellon, G. Simon, J. M. De Teresa, J. A. Pardo, J. Arbiol, and M. R. Ibarra, Phys. Rev. B **79**, 014431 (2009).
20) D. Venkateshvaran, W. Kaiser, A. Boger, M. Althammer, M. S. Ramachandra Rao, S. T. B. Goennenwein, M. Opel, and R. Gross, Phys. Rev. B **78**, 092405 (2008).
21) F. J. Jedema, H. B. Heersche, A. T. Filip, J. J. A. Baselmans, and B. J. van Wees, Nature **416**, 713 (2002).
22) R. L. Gao, H. W. Yang, C. L. Fu, W. Cai, G. Chen, X. L. Deng, J. R. Sun, Y. G. Zhao, and B. G. Shen, J. Alloys Compd. **624**, 1 (2015).
23) R. L. Gao, H. W. Yang, J. R. Sun, Y. G. Zhao, and B. G. Shen, Appl. Phys. Lett. **104**, 031906 (2014).
24) R. L. Gao, C. L. Fu, W. Cai, G. Chen, X. L. Deng, H. W. Yang, J. R. Sun, Y. G. Zhao, and B. G. Shen, Thin Solid Films **583**, 13 (2015).
25) S. Shimizu, K. S. Takahashi, T. Hatano, M. Kawasaki, Y. Tokura, and Y. Iwasa, Phys. Rev. Lett. **111**, 216803 (2013).
26) H. Nakayama, J. Ye, T. Ohtani, Y. Fujikawa, K. Ando, Y. Iwasa, and E. Saitoh, Appl. Phys. Express **5**, 023002 (2012).
27) S. Y. Huang, X. Fan, D. Qu, Y. P. Chen, W. G. Wang, J. Wu, T. Y. Chen, J. Q. Xiao, and C. L. Chien, Phys. Rev. Lett. **109**, 107204 (2012).
28) Y. M. Lu, Y. Choi, C. M. Ortega, X. M. Cheng, J. W. Cai, S. Y. Huang, L. Sun, and C. L. Chien, Phys. Rev. Lett. **110**, 147207 (2013).
29) R. L. Gao, Y. S. Chen, J. R. Sun, Y. G. Zhao, J. B. Li, and B. G. Shen, Appl. Phys. Lett. **101**, 152901 (2012).
30) R. L. Gao, Y. S. Chen, J. R. Sun, Y. G. Zhao, J. B. Li, and B. G. Shen, J. Appl. Phys. **113**, 183510 (2013).
31) F. Kubel and H. Schmid, Acta Crystallogr., Sect. B **46**, 698 (1990).
32) J. X. Zhang, Q. He, M. Trassin, W. Luo, D. Yi, M. D. Rossell, P. Yu, L. You, C. H. Wang, C. Y. Kuo, J. T. Heron, Z. Hu, R. J. Zeches, H. J. Lin, A. Tanaka, C. T. Chen, L. H. Tjeng, Y. H. Chu, and R. Ramesh, Phys. Rev. Lett. **107**, 147602 (2011).
33) P. A. Lee and T. V. Ramakrishnan, Rev. Mod. Phys. **57**, 287 (1985).
34) M. Suzuki, H. Muraoka, Y. Inaba, H. Miyagawa, N. Kawamura, T. Shimatsu, H. Maruyanma, N. Ishimatsu, Y. Isohama, and Y. Sonobe, Phys. Rev. B **72**, 054430 (2005).
35) S. R. Shinde, S. BOgale, J. S. Higgins, H. Zheng, A. J. Millis, V. N. Kulkarni, R. Ramesh, R. L. Greene, and T. Venkatesan, Phys. Rev. Lett. **92**, 166601 (2004).
36) V. T. Volkov, V. I. Levashov, V. N. Matveev, and V. A. Berezin, Appl. Phys. Lett. **91**, 262511 (2007).